Research Square

Preprints are preliminary reports that have not undergone peer review.
They should not be considered conclusive, used to inform clinical practice,
or referenced by the media as validated information.

Fabrication of Fluorine Doped Ti/SnO2-Sb/α-PbO2/F-doped β-PbO2 Electrode and Optimized Treatment of Dye Wastewater Using Response Surface Methodology in Plate and Frame Electrolytic Cell

lianyan zhu
Nanjing Polytechnic Institute
xf zhou
zhouxf@njtech.edu.cn
Nanjing Tech University

Research Article

Keywords: F-doped β-PbO2 electrode, wastewater, response surface method, electrochemical oxidation

Posted Date: April 18th, 2026

DOI: https://doi.org/10.21203/rs.3.rs-9290616/v1

License: This work is licensed under a Creative Commons Attribution 4.0 International License.
Read Full License

Fabrication of Fluorine Doped Ti/SnO_2-Sb/α-PbO_2/F-doped β-PbO_2 Electrode and Optimized Treatment of Dye Wastewater Using Response Surface Methodology in Plate and Frame Electrolytic Cell

ZHU Lian-yan[1]，ZHOU Xing-fu[2*]

[1]Department of Education and Science, Nanjing Polytechnic Institute, Nanjing, 210048; [2]State Key Laboratory of Materials-Oriented Chemical Engineering, College of Chemistry and Chemical Engineering, Nanjing Tech University, Nanjing, 210009, China

*Corresponding author: E-mail address: zhouxf@njtech.edu.cn (Prof. X.F. Zhou)

Abstract Metal-oxide electrode with high catalytic performance and good corrosion resistance is the core of electrochemical oxidation. PbO_2 electrodes have a long service life, excellent electrocatalytic stability and electrochemical corrosion resistance. Electrochemical treatment of dyeing wastewater has many advantages, but its practical application is restricted by high energy consumption. In this paper, by optimizing the NaF doping concentration, the β-PbO_2 electrode with the best decolorization performance for methylene blue wastewater was prepared, and the prepared electrode has the highest oxygen evolution potential of 1.81V and the longest accelerated life of 32 h. The optimized PbO_2 electrode was used in a plate frame electrolytic cell to treat methylene blue wastewater, and the electrolytic conditions were optimized to reduce energy consumption. The quadratic multivariate fitting model of electrolytic conditions on decolorization rate and energy consumption was established by the response surface method. The experimental results show that the fitting effects of the two models were good, and the adjusted R^2 square was greater than 0.99. The Pareto solution set was obtained by the NSGA-III algorithm. The optimized operation condition with the lowest energy consumption was investigated and listed as follows: current density is 9.37 mA/cm^2, electrolyte concentration is 0.025 M, pH value is 6.37 and electrolytic time is 10 min. The optimized energy consumption per ton of wastewater treatment is 4.60 kWh.

KEYWORDS: F-doped β-PbO_2 electrode; wastewater; response surface method；electrochemical oxidation

1. Introduction

Methylene blue (MB) is a water-soluble dye, which is widely used in the dyeing industry. Untreated MB dye wastewater discharged outward will cause harm to aquatic organisms. Excessive exposure to this pollutant will also cause anemia, nausea and vomiting[1-3]. A variety of processes based on physical, chemical and biological technologies have been used to remove dyes from wastewater. In recent years, electrochemical anodic oxidation method has attracted extensive attention due to its advantages of easy operation, high efficiency and environmental compatibility[4-6]. However, its industrial development has been restricted by its high energy consumption. The main factors affecting the efficiency and energy consumption of electrochemical anodic oxidation method include anode material, electrolyte type, current density, reactor structure, electrode spacing, pH of wastewater, etc.

Anode materials with high oxygen evolution overpotential, high catalytic performance and good corrosion resistance are the core of electrochemical anodic oxidation. PbO_2 electrode is an inert anode that can generate hydroxyl radicals in situ, and has been widely studied for the treatment of phenols, dyes and other toxic chemicals[7-11]. Compared with other electrodes, PbO_2 electrode has stable catalytic oxidation performance, long service life and low preparation cost. Compared with traditional RuO_2 and IrO_2 electrodes, PbO_2 electrode has higher oxygen evolution potential (OEP), which can not only reduce energy consumption caused by oxygen evolution in electrolysis process, but also improve current efficiency[12]. In addition, PbO_2 electrode has the advantages of long service life and good catalytic oxidation stability. Although fluorine doping has been applied to the electroplating preparation of PbO_2 electrode to prolong its service life and degradation capacity[13], the concentration of NaF doped in the preparation of PbO_2 electrode is different in each research, usually between 0.5-2 g/L[14, 15]. The pollutants and degradation conditions treated by PbO_2 electrode are also different in each research. Therefore, it is difficult to find the specific impact of fluorine ion doping concentration on the performance of PbO_2 electrode in the treatment of methylene blue wastewater.

In order to enhance the efficiency and practicality of electrochemical processes, it is crucial not only to employ anodes with superior performance but also to model and optimize electrolytic conditions for the electrochemical oxidation of wastewater. In recent years, many researchers have

conducted experimental design, modeling and optimization for wastewater degradation[16-21], but they have not considered the energy consumption cost and the high energy consumption is the most important reason which limit its industrialization[22].

The plate and frame electrolytic cell have small pole spacing and uniform current distribution, which is conducive to reducing energy consumption and secondary reaction. It can also realize the continuous treatment of wastewater through appropriate amplification, series, parallel and other designs. It is the most widely used chemical treatment reactor for wastewater. In this paper, we first optimized the concentration of NaF doping and prepared the Ti/SnO_2-Sb/α-PbO_2/β-PbO_2 electrode with the best decolorization effect on MB wastewater, the optimized PbO_2 electrode was used in a plate and frame reactor to treat low concentration and low salt MB wastewater by electrochemical oxidation, then the linear regression models of electrolysis conditions on decolorization rate and energy consumption were established by response surface design, the Pareto front solution set of color removal rate and minimum energy consumption was obtained by NSGA-III genetic algorithm, and the solution of the operation condition that the decolorization rate of MB wastewater reached 95% and the minimal energy consumption was realized. The optimized operation condition with the lowest energy consumption was investigated and listed as follows: current density was 9.37 mA/cm^2, electrolyte concentration was 0.025 M, pH value was 6.57 and electrolytic time was 10 min. The optimized energy consumption per ton of wastewater treatment was 4.60 kWh.

2. Experimental

2.1 Materials and instruments

Titanium plate (purity > 99.5%) was purchased from Nanjing Tang Nonferrous Metal Industrial Co., Ltd (China). Chemicals were analytical reagent grade and used as supplied. The morphologies of PbO_2 electrode were observed on a FEI Quanta-200 0Scanning electron microscopy (SEM). Surface composition of the electrode coatings was determined on a Bruker-D8Advance X-ray diffractometer with graphite monochromatized high-intensity Cu Kα radiation at 40KV and 30mA.

2.2 Preparation and characterization of electrodes

Before the experiment, we need to pretreat the titanium plate. In the process of pretreatment,

the surface of titanium sheet is simply polished with sandpaper, soaked in 60 ℃ NaOH solution for 20 minutes, and then ultrasonically treated in absolute ethanol and deionized water for 30 minutes. The titanium sheet (4 cm×5 cm×0.05 cm) in 10 wt.% oxalic acid solution for 150 minutes at 98 ℃. Isopropanol solution contains $SnCl_4 \cdot 5H_2O$ and $SbCl_3$ with a molar ratio of 10:1 was brush on the titanium substrate, dry in 100 °C oven for 10 minutes, and then calcine in 500 °C muffle furnace for 10 minutes. The process was repeated 10 times, and the last time was annealed at 500 °C for 60 minutes. The α-PbO_2 layer was prepared by electroplating in the solution containing 0.1 M PbO and 3.5 M NaOH with the current density of 3 mA/cm^2, and the electroplating time was 1 h. The β-PbO_2 layer was prepared in the solution containing 0.5 M $Pb(NO_3)_2$, 0.1 M HNO_3, 0.1 M Cu $(NO_3)_2$ and NaF (0.5g/L, 1 g/L, 1.5 g/L, 2 g/L) with the current density of 20 mA/cm^2 in the temperature of 60 ℃. and the plating time was 1 h. The electrodes were prepared using different NaF concentrations of 0.5 g/L 1 g/L, 1.5 g/L and 2 g/L and were recorded as 0.5-NaF, 1-NaF, 1.5-NaF and 2-NaF respectively.

The morphologies of the anodes were analyzed by a field emission scanning electron microscopy (SEM, Hitachi-s800, Japan). X-ray diffraction (XRD) patterns were obtained in the radiation range of 20° − 80° with the scanning rate of 10 min^{-1} on D-Max diffractometers to study the crystal structure of the electrode. All the electrochemical analysis including cyclic voltammograms (CV), linear sweep voltammetry (LSV), and electrochemical impedance spectroscopy (EIS) were performed at the three-electrode electrochemical workstation (CHI660D, Shanghai Chenhua Instrument Co., Ltd., China), in which the anode, platinum plate and saturated calomel electrode (SCE) were used as working electrode, counter electrode and reference electrode, respectively.

2.3 Electrochemical reactor setup

The electrolytic decolorization is carried out in a plate and frame electrolytic cell, as shown in Fig.1. Both anode and cathode were separated from each other by 1.2 cm distance in a vertical position. For each electrochemical assay, 160 mL of MB solution was used. The electrolysis was conducted under galvanostatic mode employing a regulated Direct Current (DC) from power supply (model E). Two sheets of Ti/SnO_2-Sb/α-PbO_2/β-PbO_2 were used as anode, while the steel sheet was used as counter electrode. The effective surface area of both electrodes was 80 cm^2 (20 cm^2 on each

face side). The spectrophotometer is used to determine the absorbance of dye wastewater, and the decolorization rate of dye wastewater is calculated according to formula 1, where A1 and A2 are the absorbance of characteristic peak (664 nm) of MB before and after treatment.

$$\text{Color removal rate} = \frac{\text{A1} - \text{A2}}{\text{A1}} \times 100 \quad (1)$$

The energy consumption (EC) is the electric energy required for equivalent treatment of 1 ton of wastewater in each batch, which is calculated by the following formula 2.

$$\text{Energy consumption} = \frac{U \times I \times t}{V/1000} \quad (2)$$

Where U is the average voltage (V), I is the current (A), t is the electrolysis time (h) and V is the solution volume (L).

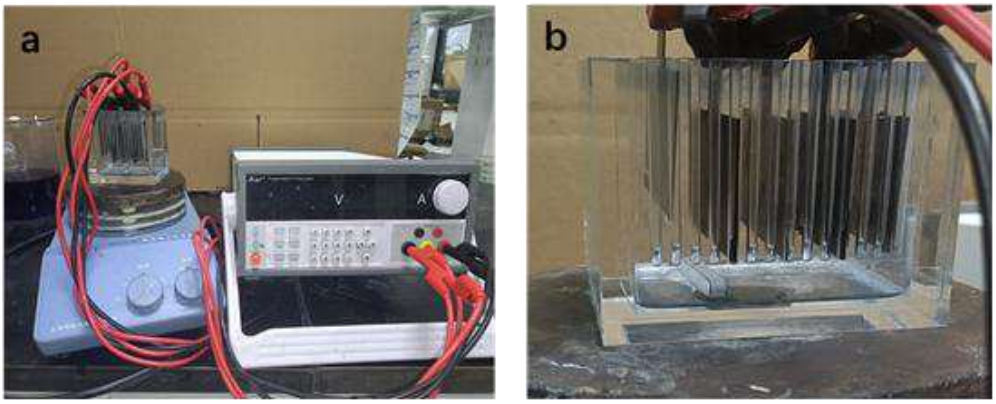


Fig.1 plate and frame electrolytic cell

2.4 Experimental design, multiple linear regression (MLR) modelling & optimization

The experimental procedure for the batch MB dye abetment and subsequent EC process was designed using a central composite design (CCD) implemented via the Design Expert software, in accordance with widely adopted methodologies. In this work, color removal rate and EC were set as simultaneous responses, while estimators were pH, current density, supporting electrolyte (Na_2SO_4) concentration and treatment time. Polynomial models predicting the relationship between variables and responses were developed using the multiple linear regression (MLR) technique. These models were evaluated based on Analysis of Variance (ANOVA) and regression coefficients (R^2, adjusted R^2 adj, predicted R^2). Model validation was conducted using sequential F-tests, p-values, and lack-of-fit tests.

3. Result and discussion

3.1 Characterizations of the anodes

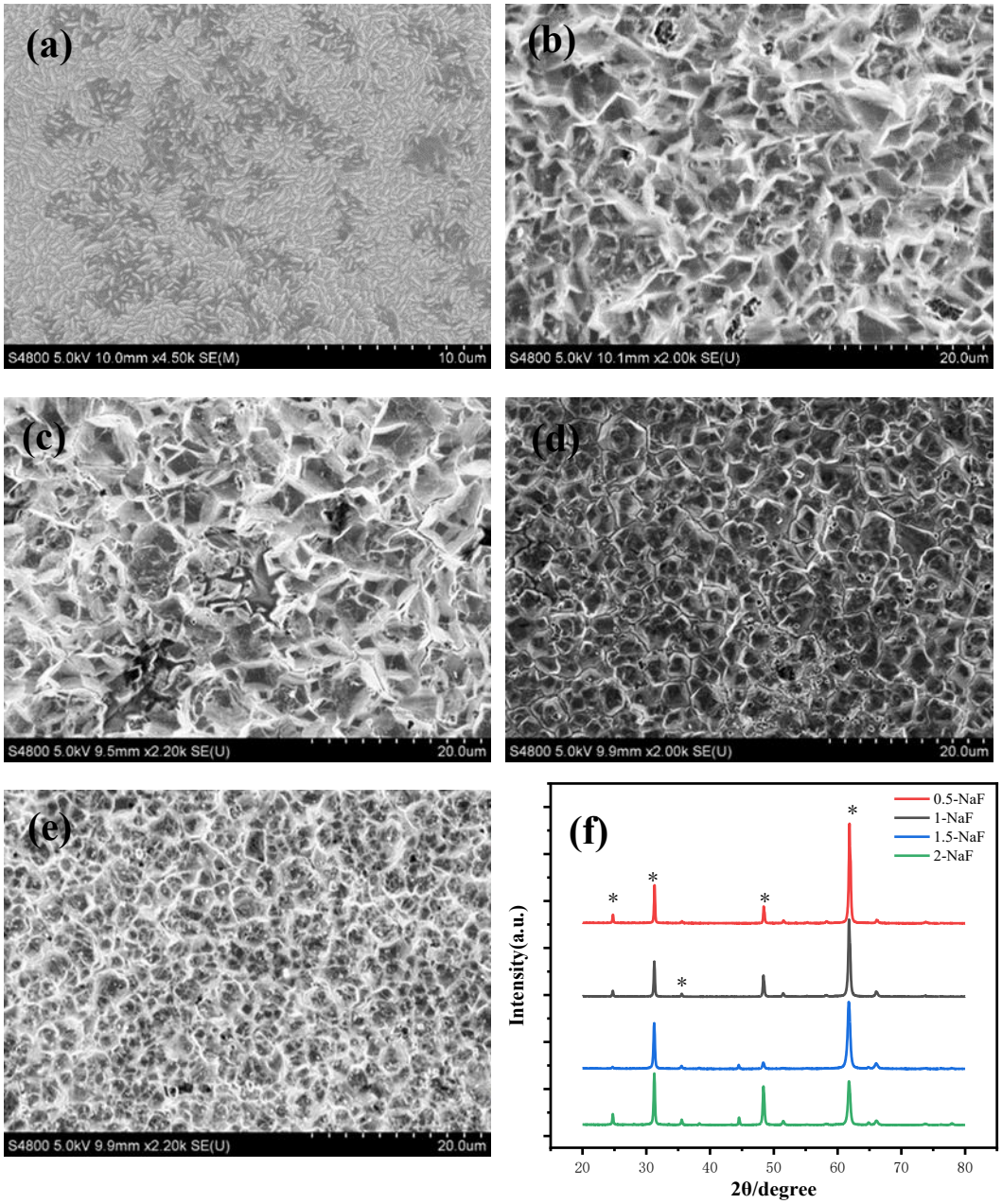


Fig.2 SEM images and XRD of different electrodes: (a) α-PbO_2 layer (b) 0.5-NaF doped β-PbO_2 (c) 1-NaF doped β-PbO_2 (d) 1.5-NaF doped β-PbO_2 (e) 2-NaF doped β-PbO_2 (f) XRD of different β-PbO_2

SEM images of the PbO_2 electrodes with different NaF amount were compared in Fig.2. It can be seen that the surfaces of 0.5-NaF and 1-NaF electrodes are typical irregular cubic conical

structures, which is consistent with the morphology reported in the literature. When the NaF concentration was within 1g /L, the electrode morphology did not change significantly with the increase of NaF concentration. When NaF concentration reaches 1.5 g/L, the cubic cone structure of β-PbO_2 crystal disappears, the grain size decreases and there is an obvious boundary between the grains. With the further increase of NaF concentration, the edges and corners of β-PbO_2 crystal disappear and become hemispherical, and the phase clusters between crystals.

Table 1 Lattice parameters of different β-PbO_2

Electrode	2θ	FWMH	Average size（nm）
0.5-NaF	61.898	0.372	47.44
1-NaF	61.829	0.405	43.58
1.5-NaF	61.812	0.466	37.81
2-NaF	61.773	0.527	33.38

Fig.2(f) shows the XRD pattern of β-PbO_2 active layer, The main diffraction peaks of PbO_2 at 24.7°, 31.3°, 35.6°, 48.4° and 61.9° belong to (110), (101), (200), (211) and (301) crystal planes. The positions of the diffraction peaks are basically consistent with the standard data of JCPDS card (pdf\76 – 0564). As can be seen from Fig.2 (f), with the increase of NaF concentration, The (301) plane diffraction peak of β-PbO_2 grain gradually decreases while the (101) plane diffraction peak gradually increases. The average crystallite size of β-PbO_2 was calculated using the Debye–Scherrer formula (Formula 3) and is presented in Table 1. In this formula, θ represents the Bragg diffraction angle, B denotes the full width at half maximum (FWHM) of the peak, K is the crystallite shape constant (0.943), and λ corresponds to the X-ray wavelength (0.15406 nm). The resulting values are summarized in Table 1.

$$D = \frac{k\lambda}{B * cos\theta} \quad (3)$$

With the increase of NaF concentration, the grain size of β-PbO_2 decreases. A smaller particle size is conducive to the formation of a larger effective area, which can improve the catalytic performance of the electrode [23].

3.1.2. Electrochemical performance of the anodes

The higher the oxygen evolution potential (OEP) of the electrode, the lower the probability of oxygen evolution side reaction[24]. As shown in Fig.3 (a), the LSV curves illustrate the oxygen evolution process of the electrode. The oxygen evolution potential of the electrode is the intersection of the tangent of the oxygen evolution current and the horizontal axis. It can be observed that the 1.5-NaF electrode exhibits the highest OEP value of 1.81 V among all samples.

Fig. 3(b) presents the CV curves of the different electrodes recorded in 0.1 M Na_2SO_4 solution. As can be seen, the 0.5-NaF, 1-NaF, and 1.5-NaF electrodes each exhibit an oxidation peak between 1.1 V and 1.3 V, along with a corresponding reduction peak in the range of 0.8 V to 0.9 V. This oxidation-reduction peak corresponds to the oxidation-reduction of Pb^{2+} and Pb^{4+}. At the same time, it can be observed that the 1.5-NaF electrode has the highest oxidation peak current density of 2.41 mA/cm^2, which indicates that the 1.5-NaF electrode has the largest active surface area and provides more active sites for electrochemical reactions.

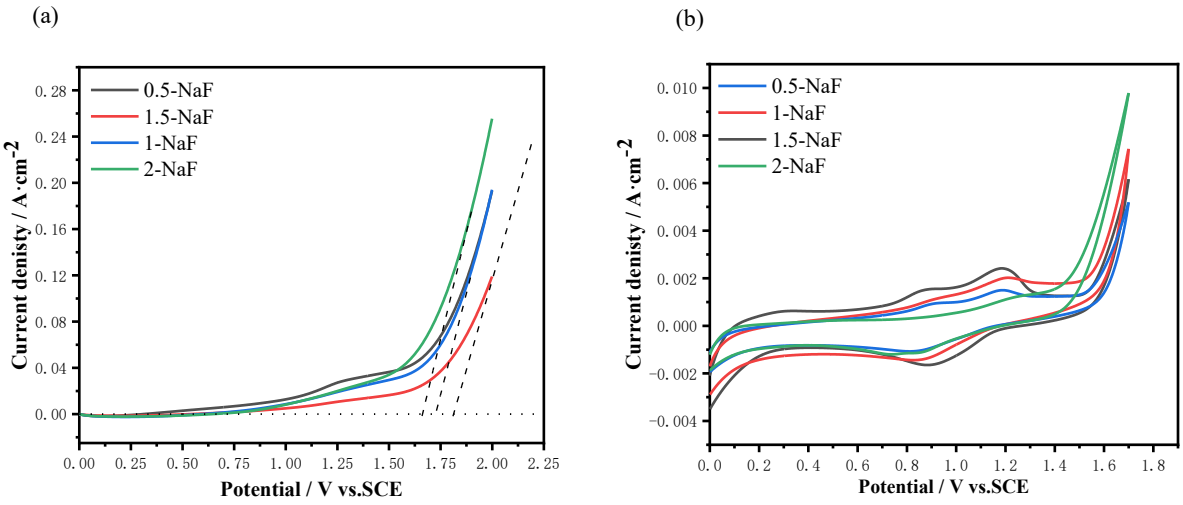


Fig.3 (a) LSV curves of the different electrodes(b) LSV curves of the different electrodes

Fig. 4 presents the CV curves of the 1.5-NaF electrode in methylene blue solutions at different concentrations (0 ppm, 10 ppm, and 100 ppm). Compared to the blank solution, no additional peaks are observed in the presence of methylene blue, suggesting that no direct electron transfer occurs between the electrode and the dye molecules. Therefore, the degradation of methylene blue in this system is likely achieved through indirect oxidation processes [25].

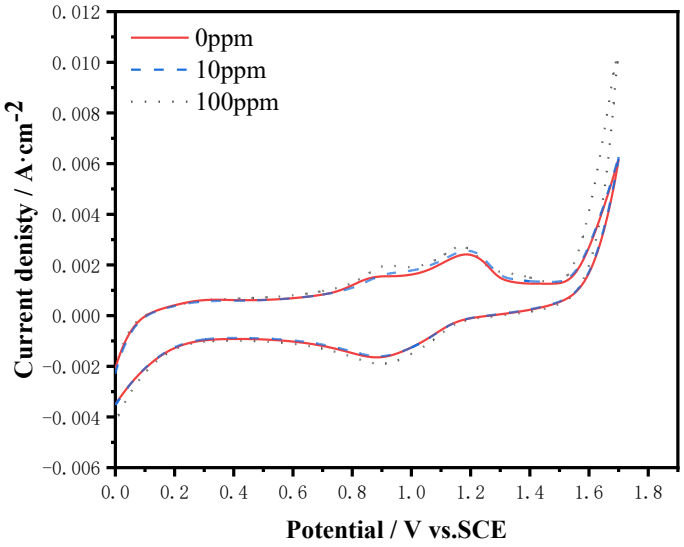


Fig.4 CV curves of 1.5-NaF electrode in different concentrations of methylene blue (0 ppm, 10 ppm, 100 ppm) solutions

Fig.5 shows the Nyquist diagram of different electrodes in the frequency range of 0.01 – 10^5 Hz. And the Nyquist diagram of all electrodes presents a semicircle with a certain radius. The Nyquist spectra were interpreted using an equivalent circuit model, the intersection of the high-frequency end and the real axis is the solution resistance R_s, the semicircle diameter represents the charge transfer resistance R_{ct}, and C_{dl} represents the electric double-layer capacitance formed between the electrode surface and the electrolyte. The equivalent circuit fitting results for each electrode are summarized in Table 2.

As shown in Table 2, the solution resistance R_s of the four electrodes is relatively similar, whereas notable differences are observed in the charge transfer resistance R_{ct}. The charge transfer resistance R_{ct} increases gradually in the order of 0.5-NaF, 1-NaF, and 1.5-NaF electrodes, and the more obvious the charge transfer resistance R_{ct} is, the easier the chemical reaction, that is, the oxygen evolution reaction, occurs in the interface layer between the electrode and the solution, which indirectly explains the reason for the highest oxygen evolution potential of 1.5-NaF electrode. The R_{ct} of 2-NaF electrode is much smaller than that of 0.5-NaF electrode. The possible reason is that excessive NaF will lead to the formation of high conductivity PbF_2 and faster interfacial charge transfer.

Table 2 Impedance fitting data of electrodes

Electrode	R_{ct}/Ω	R_s/Ω	C/mF·cm^{-2}
0.5-NaF	12.70	7.02	1.88

1-NaF	25.30	6.21	0.67
1.5-NaF	38.30	7.16	0.49
2-NaF	7.90	7.30	0.12

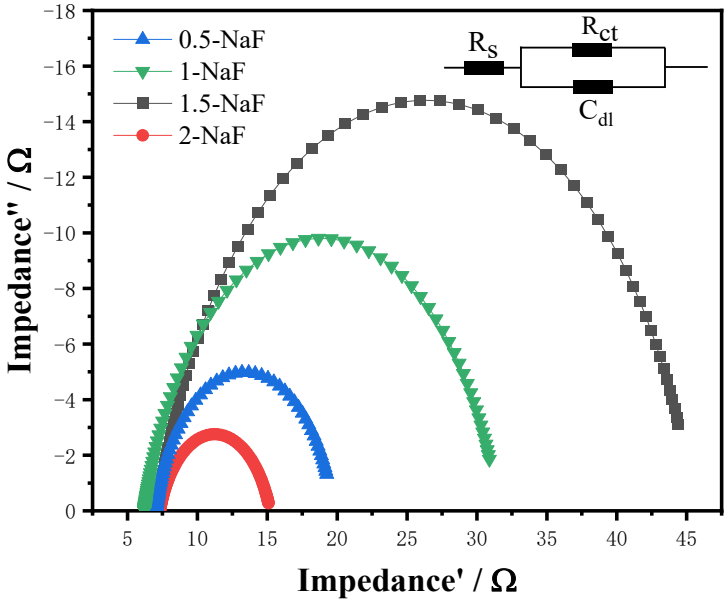


Fig.5 EIS diagrams of electrodes and analog circuit component diagram

Fig.6 (a) and (c) show the time-varying curves of the removal rates of MB and methyl orange (MO) in wastewater by each electrode. It can be clearly seen that each electrode can decolorize and degrade pollutants almost completely, but the time required is significantly different. Among them, 1.5-NaF electrode showed the best performance in both the degradation of the dye wastewater. The decolorization rate of MB reached 98.5% at 25 min and that of MO reached 96.1% at 15 min. However, the electrocatalytic oxidation performance of 2-NaF electrode does not improve with the increase of NaF doping concentration, instead, it is significantly lower than that of 0.5-NaF electrode. This is because the oxygen evolution potential of 2-naf electrode is the lowest, and the oxygen evolution reaction is more likely to compete with the main reaction in the electrolysis process.

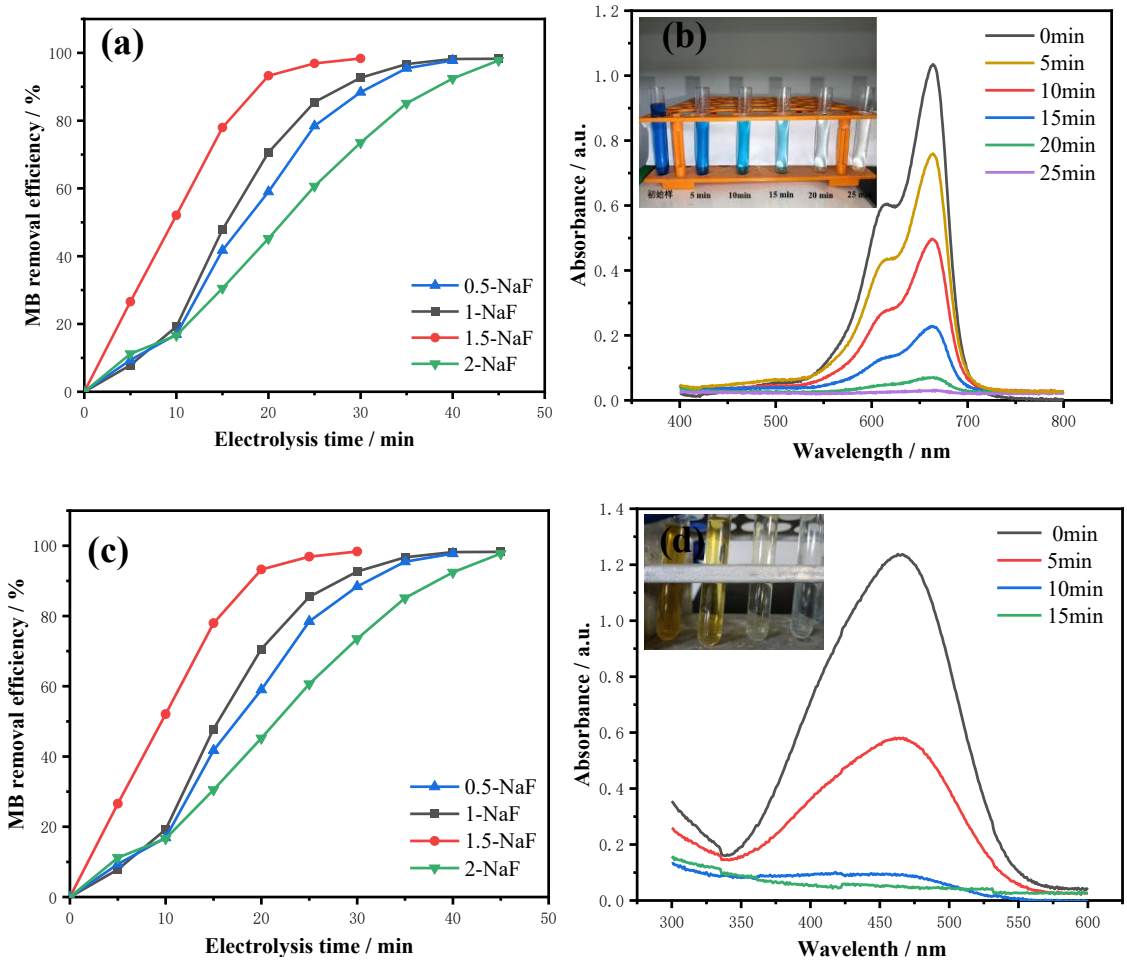


Fig.6 Degradation curve of 20 ppm dye wastewater by different electrodes: (a) MB (b) UV-Vis absorption spectra of the MB wastewater (c) MO (d) absorption spectra of the MO wastewater

Fig.7 shows the change curve of cell voltage value with time during the test of each electrode. The stability of each electrode was tested in 1.0 mol/l H_2SO_4 solution with a current density of 2 A/cm^2. It can be seen from the figure that the cell pressure of each electrode was about 6.8 V at the beginning of the test, and a sharp rise in the cell pressure was observed in the last few hours. As shown in the fig.7, the 1.5-NaF electrode showed a longest accelerated life of 32 h.

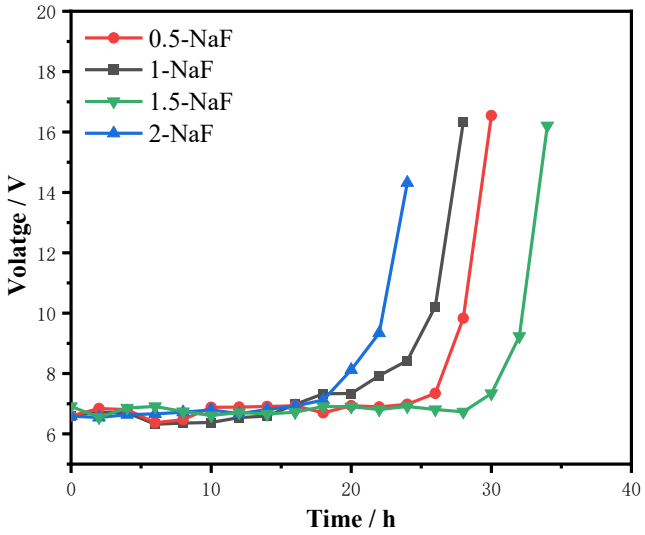


Fig.7 Accelerated life test curves of different electrodes

3.2 Process optimization

According to the experimental design principles, four factors that affect the decolorization rate and energy consumption are selected: current density (X_1), electrolyte concentration (X_2), pH value (X_3) and electrolysis time (X_4). Each of the five levels is recorded as level -2, -1, 0, 1 and 2, as shown in Table 3. The response surface analysis test of 30 test points at the factor level, including 6 center points, was conducted to evaluate the actual experimental error. The experimental results obtained according to the central composite design are listed in Table 4.

Table 3 Level and code of experimental variables based on the central composite design

Parameters		**Levels**				
		-2	-1	0	1	2
current density (mA/cm^2)	X_1	4	8	12	16	20
lectrolyte concentratio(Na_2SO_4) (mol / L)	X_2	0.005	0.01	0.015	0.02	0.025
pH value	X_3	3	5	7	9	11
electrolysis time (min)	X_4	2	4	6	8	10

Table 4 Experimental design and results in central composition design

	X_1	X_2	X_3	X_4	decolorization rate(Y_1)		energy consumption(Y_2)	
umber	urrent denisty (mA/cm^2)	electrolyte concentration (M)	pH	ectrolysis time (min)	real	predict	real	predict
1	12	0.015	3	6	50.63	51.31	4.15	4.13
2	8	0.010	5	8	60.11	59.02	3.77	3.99

3	12	0.015	7	6	71.82	72.70	4.51	4.39
4	12	0.015	7	10	98.42	99.11	7.42	7.47
5	16	0.020	5	8	98.56	98.86	8.01	8.03
6	8	0.010	5	4	34.21	33.71	1.95	1.90
7	8	0.020	9	8	67.12	66.16	2.95	2.80
8	16	0.020	9	8	94.11	93.73	7.96	8.02
9	16	0.010	5	8	96.06	96.22	11.00	10.85
10	16	0.020	5	4	62.80	62.37	4.18	3.98
11	4	0.015	7	6	34.52	37.07	0.81	0.61
12	12	0.015	7	6	72.07	72.70	4.25	4.39
13	20	0.015	7	6	96.00	95.24	9.71	9.82
14	16	0.020	9	4	60.03	60.21	4.14	4.00
15	12	0.015	7	6	73.07	72.70	4.45	4.39
16	8	0.020	5	4	38.58	37.68	1.48	1.65
17	16	0.010	5	4	64.25	64.30	5.65	5.89
18	12	0.015	7	2	39.17	40.27	1.49	1.35
19	8	0.020	9	4	40.28	39.24	1.48	1.64
20	12	0.015	7	6	73.58	72.70	4.47	4.39
21	8	0.010	9	4	41.07	39.86	1.95	2.01
22	16	0.010	9	8	95.70	95.68	11.05	10.96
23	12	0.025	7	6	73.14	74.23	4.10	4.25
24	12	0.015	7	6	72.66	72.70	4.46	4.39
25	12	0.015	11	6	51.21	52.32	4.31	4.24
26	8	0.020	5	8	68.31	67.57	2.95	2.83
27	12	0.005	7	6	71.51	72.21	7.67	7.44
28	8	0.010	9	8	62.64	62.20	3.88	4.08
29	16	0.010	9	4	66.87	66.73	5.90	6.03
30	12	0.015	7	6	73.01	72.70	4.21	4.39

Using design expert 10.0 data analysis software, multiple linear regression fitting is carried out with decolorization rate (Y_1) and energy consumption (Y_2) as response values, and the quadratic multiple regression coding equations of decolorization rate and energy consumption are obtained as follows:

$$Y_1 = 72.7 - 14.54X_1 - 0.51X_2 + 0.25X_3 + 14.71X_4 - 1.64X_1^2 - 0.13X_2^2 - 5.22X_3^2 - 0.75X_4^2 - 1.49X_1X_2 - 0.93X_1X_3 + 1.65X_1X_4 - 1.15X_2X_3 + 1.14X_2X_4 - 0.74X_3X_4 \quad (4)$$

$$Y_2 = 4.39 + 2.3X_1 - 0.8X_2 + 0.027X_3 + 1.53X_4 + 0.21X_1^2 + 0.36X_2^2 - 0.051X_3^2 + 0.0052X_4^2 - 0.41X_1X_2 - 0.0063X_1X_3 + 0.72X_1X_4 - 0.031X_2X_3 - 0.23X_2X_4 - 0.0063X_3X_4 \quad (5)$$

Table 5 shows the analysis of variance (ANOVA) of the regression model of decolorization rate. From the table, it can be seen that the p-values of the two models are less than 0.0001, and the p-values of the lack of fit is greater than 0.05, indicating that the two models both have a good fitting degree, and can make a good prediction and analysis of the decolorization rate of MB within the range of factor selection. At the same time, the adj R^2 of the two models are both greater than 0.8000, which indicating that of the data can be explained by the model, indicating that the actual value of the model is not much different from the predicted value.

Table 5 ANOVA of MLR models for color removal (%) and energy consumption (kWh)

Source	decolorization rate (%)			energy consumption (kWh)		
	um of Squares	-value	p-value	ım of Squares	-value	p-value
Model	11216.91	63.76	< 0.0001	215.31	90.62	< 0.0001
current density(X_1)	5075.62	571.38	< 0.0001	127.33	233.96	< 0.0001
ectrolyte concentration(X_2)	6.14	4.32	0.0552	15.26	87.69	< 0.0001
PH value(X_3)	1.55	1.09	0.3128	0.0171	.4335	0.5203
electrolysis time(X_4)	5192.63	653.71	< 0.0001	56.12	425.38	< 0.0001
X_1X_2	34.93	24.58	0.0002	2.74	69.57	< 0.0001
X_1X_3	13.80	9.71	0.0071	0.0006	.0159	0.9014
X_1X_4	43.69	30.74	< 0.0001	8.21	08.48	< 0.0001
X_2X_3	21.07	14.82	0.0016	0.0156	.3969	0.5382
X_2X_4	20.93	14.73	0.0016	0.8372	21.26	0.0003
X_3X_4	8.82	6.21	0.0249	0.0006	.0159	0.9014
X_1^2	73.45	51.68	< 0.0001	1.17	29.69	< 0.0001

X_2^2	0.4621	).3251	0.5770	3.61	91.65	< 0.0001
X_3^2	747.80	;26.18	< 0.0001	0.0715	1.81	0.1979
X_4^2	15.54	10.93	0.0048	0.0007	).0189	0.8925
Lack of Fit	19.14	4.39	0.0581	0.5093	3.13	0.1097

	R^2	**ıdj R^2**	**Pred R^2**	**Std. Dev.**	**:.V. %**	**ıdeq Precision**
decolorization rate (%)	0.9981	).9963	0.9899	1.19	1.79	77.5829
:nergy consumption(kWh)	0.9973	).9947	0.9852	0.1984	4.12	73.7726

Fig. 8 illustrates the relationship between the predicted and experimental values of the two response variables: decolorization rate (%) and energy consumption. It is evident that the predicted values largely cluster around the experimental data points and are generally aligned with the line *y=x*, indicating that the prediction performance of the two models is good, which further illustrates the effectiveness of the models. The aforementioned analysis demonstrates that the models can accurately elucidate the relationship between the four factors and two response variables, respectively. Furthermore, the two models can precisely predict the optimal conditions for methylene blue decolorization and energy consumption.

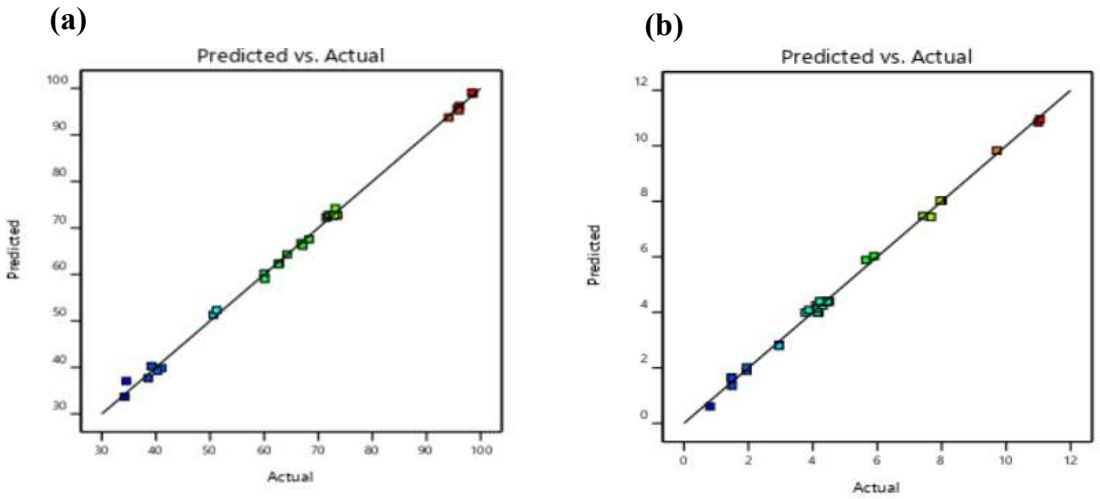


Fig.8 Plots of predicted versus observed values for MLR models; **a)-** NB degradation, **b)-** Energy consumption

Fig.9 (a) shows the effect of current density and electrolysis time on decolorization rate. It can be seen from the figure that the increase of electrolysis time and current density is helpful to improve the decolorization rate; In addition, it can be observed that with the increase of current

density and electrolysis time, the rising trend of decolorization rate gradually flattens out. This is because with the increase of current density, more oxygen evolution reactions take place at the electrode. With the increase of electrolysis time, MB dye is degraded, its concentration decreases, and the reaction rate between the free radical generated at the electrode and the dye also decreases. Fig.9 (b) shows the response surface diagram of current density and initial pH value to decolorization rate. It can be observed that under any current density, the decolorization rate reaches the maximum when the pH value is about 7. The reason is that the oxidation potential of hydroxyl radical in alkaline condition is lower than that in neutral and acidic condition; Under acidic conditions, H^+ will first combine with the central nitrogen of MB, reducing the valence of nitrogen and making MB more difficult to be oxidized. The interaction between time and electrolyte concentration on the decolorization rate is shown in Fig.9 (c). Under a long electrolysis time, the increase of electrolyte concentration can promote the decolorization rate; However, in a shorter electrolysis time, lower electrolyte concentration is beneficial to decolorization. Studies have shown that when Na_2SO_4 is used as electrolyte, electrode electrolysis will react with sulfate to form persulfate ($S_2O_8^{2-}$), thus promoting the degradation of dyes. However, the oxidation potential of persulfate is low, the reaction rate with MB is slow, but its existence time is longer. Therefore, the effect of persulfate on the decolorization of MB was not apparent until the reaction was carried out for a certain time.

Fig.9 (d) shows the response surface of current density and electrolyte concentration to energy consumption. It can be seen that the energy consumption increases with the decrease of electrolyte concentration and the increase of current density, which is consistent with the conclusions of other researchers. Obviously, when the electrolyte concentration becomes smaller, the solution resistivity between electrodes will rise, which will lead to a large amount of electrical energy being used to heat the solution between electrodes, resulting in additional energy loss. Fig.9 (e) shows the response surface of pH and current density to energy consumption. From the figure, it can be seen that pH has little effect on energy consumption, but it can be clearly observed that under non neutral conditions, energy consumption will be slightly reduced. This can be explained by analysis: adjusting pH by adding acid and alkali is equivalent to increasing the concentration of electrolyte, thus increasing the conductivity of solution and reducing energy consumption. At high current

density, the impact of pH on energy consumption is not obvious, because the impact of increasing current density on energy consumption is much greater than that of pH.

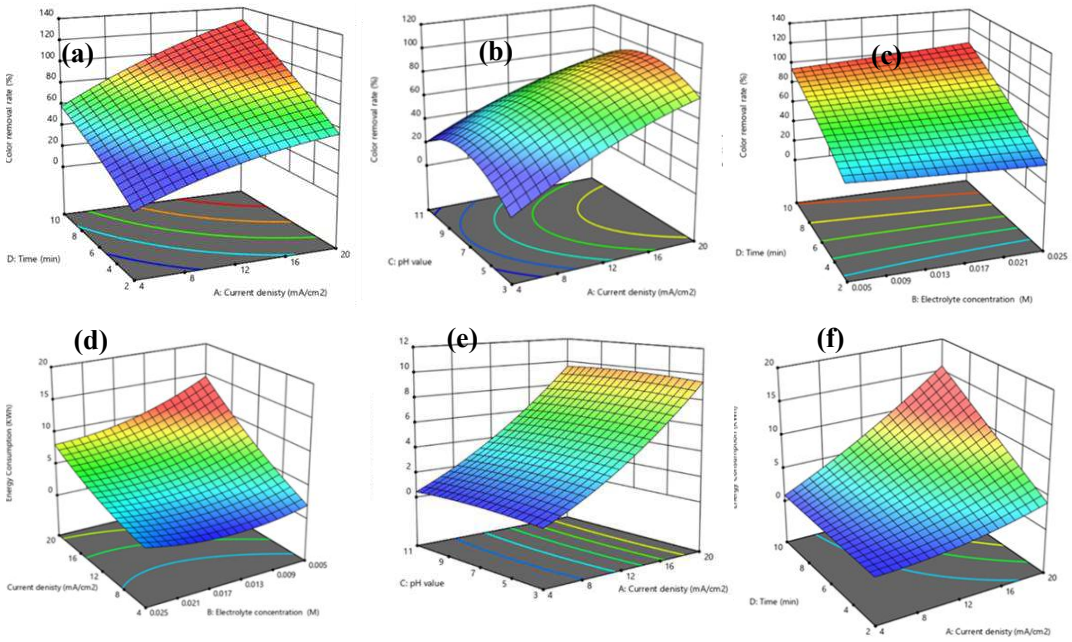


Fig. 9 Effect of variables on the MB removal rate (a-c) and energy consumption(d-f) from MLR

The R^2 of the two models of decolorization rate and energy consumption is greater than 0.99, which shows the reliability of the model. In order to find the best electrolysis conditions, in this section the electrolysis operation parameters under different decolorization rates are solved by NSGA III algorithm to minimize energy consumption [26-28]. The solution interval corresponds to the range from the minimum to the maximum value of each parameter within the central composite design. The population size is set to 300 and the number of iterations is set to 100.

Fig. 10 shows the Pareto front graph of decolorization rate and energy consumption, in which the blue dot is the Pareto optimal solution obtained by NSGA III algorithm. From the periphery of the design space, an optimal envelope can be obtained by approximate extreme solution, which is called Pareto optimal Frontier (gray dotted line). Under the Pareto optimal frontier, we can find a better optimization scheme than the optimal solution, but these combinations cannot be realized in the design space.

It can also be observed from Fig. 10 that the relationship between decolorization rate and

energy consumption is divided into two stages. When the decolorization rate is lower than 65%, the energy consumption does not change significantly with the increase of decolorization rate, and the required energy consumption is less than 1 kwh; When the decolorization rate reaches more than 65%, any further increase of the decolorization rate leads to a significant rise in energy consumption. The optimization in this paper includes two objectives, the decolorization rate is more than 95%, and the energy consumption is the minimum when the decolorization rate is reached. The target and the points near the target are marked in the red circle, and their solutions are listed in Table 6.

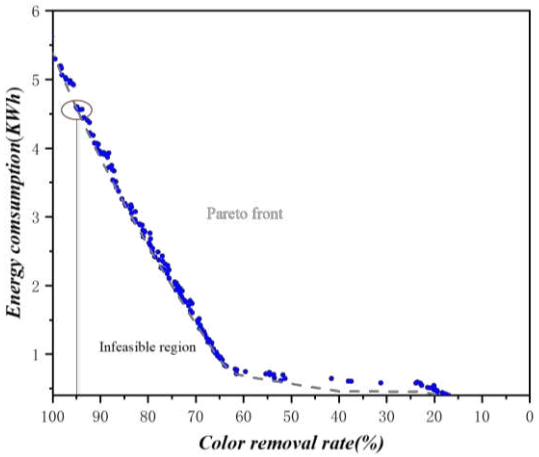


Fig.10 Pareto frontier diagram of decolorization rate and energy consumption

Table 6 Solution set in red circle

current density （mA/cm^2）	electrolyte concentration (M)	pH value	Electrolysis time(min)	color removal rate (%)	nergy onsumption kWh)
9.31	0.0250	6.60	10	94.83	4.56
9.37	0.0250	6.37	10	95.12	4.60
9.44	0.0250	6.57	10	95.40	4.64
9.51	0.0250	6.65	10	95.67	4.69
9.56	0.0250	6.50	10	95.94	4.72
9.67	0.0249	6.72	10	96.21	4.79

It can be seen from Table 6 that when the current density, electrolyte concentration, pH value and electrolysis time are 9.37 mA/cm^2, 0.025 M, 6.37 and 10 min respectively, the optimization goal is reached. At this time, the decolorization rate of MB is 95.12% and the energy consumption is 4.60 kwh. Subsequently, we tested and verified the optimization results. Under these operating

parameters, the real decolorization rate of MB was 95.92%, the real tank pressure was 5.95 V, and the calculated energy consumption was 4.65 kWh, which was not much different from the results obtained through model optimization.

4. Conclusion

We optimized the Ti/SnO_2-Sb/α-PbO_2/β-PbO_2 electrode by controlling the NaF concentration in the plating solution. When the concentration of NaF was 1.5 g/l, the prepared electrode had the best electrochemical performance. The electrode showed a oxygen evolution potential of 1.81 V, which higher than other electrodes. The optimized PbO_2 electrode is used in the plate and frame electrolytic cell to simulate the industrial application scenario to optimize the operating parameters. The real test data were obtained through the central composite test design, and the linear regression model of influencing factors on decolorization rate and energy consumption was established. The mismatch terms of the two models were not significant, and the regression coefficient R^2 was greater than 0.99. The model has a good ability to predict and explain the real results. Through NSGA- III algorithm, the operating conditions with decolorization rate greater than 95% and lowest energy consumption are obtained: current density of 9.37 mA/cm^2, electrolyte concentration of 0.025 M, pH of 6.37 and electrolysis time of 10 min. At this time, the predicted energy consumption is 4.6 kWh per ton of wastewater, which is not much different from the real test result of 4.65 kWh.

Reference

[1] M. Fayazi, M. A. Taher, D. Afzali, et al, Enhanced Fenton-like degradation of methylene blue by magnetically activated carbon/hydrogen peroxide with hydroxylamine as Fenton enhancer, Journal of Molecular Liquids. (2016). https://doi.org/10.1016/j.molliq.2016.01.093.

[2] D. Pathania, S. Sharma, P. Singh, Removal of methylene blue by adsorption onto activated carbon developed from Ficus carica bast, Arabian Journal of Chemistry. (2013). https://doi.org/10.1016/j.arabjc.2013.04.021.

[3] Q. Li, Y. Li, X. Ma, Filtration and adsorption properties of porous calcium alginate membrane for methylene blue removal from water, Chemical Engineering Journal. (2017). https://doi.org/10.1016/j.cej.2017.01.098.

[4] S. Pulkka, M. Martikainen, A. Bhatnagar, Electrochemical methods for the removal of anionic contaminants from water - A review, Separation & Purification Technology. (2014). https://doi.org/10.1016/j.seppur.2014.05.021.

[5] D. B. Miklos, C. Remy, M. Jekel, et al, Evaluation of advanced oxidation processes for water and wastewater treatment - A critical review, Water Research. (2018). https://doi.org/10.1016/j.watres.2018.03.042.

[6] M. Zhang, Q. Shi, X.Z. Song, et al, Recent electrochemical methods in electrochemical degradation of halogenated organics: a review, Environmental Science and Pollution Research. (2019). https://doi.org/10.1007/s11356-019-04533-3.

[7] D. Bejan, E. Guinea, N. J. Bunce, On the nature of the hydroxyl radicals produced at boron-doped diamond and Ebonex anodes, Electrochimica Acta. (2012). https://doi.org/10.1016/j.electacta.2012.02.097.

[8] S. Saaidia, R. Delimi, Z. Benredjem, et al, Use of a PbO_2 electrode of a lead-acid battery for the electrochemical degradation of methylene blue, Separation Science and Technology. (2017). https://doi.org/10.1080/01496395.2017.1291681.

[9] W. Ji, Y. Xiong, Y. Wang, et al, Multilayered TNAs/SnO2/PPy/beta-PbO2 anode achieving boosted electrocatalytic oxidation of As (III). Journal of Hazardous Materials. 2022）. https://doi.org/.1016/j.jhazmat.2022.128449

[10] Y. F. Pan, Y. F. Luo, C. C. Li, et al, Preparation and characterization of Ti/SnO_2-Sb2O3/α-PbO2/Ce-Nd-β-PbO2 composite electrode for methyl orange degradation, Journal of Solid State Electrochemistry. (2020). https://doi.org/10.1007/s10008-019-04468-2.

[11] Q. Q. Zhou, X. L. Zhou, R. H. Zheng, et al, 2021. Application of lead oxide electrodes in wastewater treatment: A review. Science of The Total Environment. (2021). https://doi.org/10.1016/j.scitotenv.2021.150088.

[12] X. Zhou, Q. Zhou, H. Chen, et al, Influence of dimethylphenol isomers on electrochemical degradation: Kinetics, intermediates, and DFT calculation. Science of The Total Environment, (2021). https://doi.org/10.1016/j.scitotenv.2021.148284.

[13] J. Cao, H. Zhao, F. Cao, et al, The influence of F- doping on the activity of PbO2 film electrodes in oxygen evolution reaction, Electrochimica Acta. (2007). https://doi.org/10.1016/j.electacta.2007.06.038.

[14] A. Ansari, D. Nematollahi, Convergent paired electrocatalytic degradation of p-dinitrobenzene by Ti/SnO2-Sb/β-PbO2 anode. A new insight into the electrochemical degradation mechanism. Applied Catalysis B-Environmental. (2019). https://doi.org/10.1016/j.apcatb.2019.118226.

[15] Y. S. Chen, D. X. Liao, Y.Lin, et al, 2022. Electrochemical degradation performance and mechanism of dibutyl phthalate with hydrophobic PbO2 electrode. Chemosphere. (2022). https://doi.org/10.1016/j.chemosphere.2021.132638.

[16] G. Bonyadinejad, M. Sarafraz, M. Khosravi, et al, Electrochemical degradation of the Acid Orange 10 dye on a Ti/PbO_2 anode assessed by response surface methodology, Korean Journal of Chemical Engineering. (2016). https://doi.org/10.1007/s11814-015-0115-x.

[17] K. Rajkumar, M. Muthukumar, Optimization of electro-oxidation process for the treatment of Reactive Orange 107 using response surface methodology, Environmental Science and Pollution Research. (2012). https://doi.org/10.1007/s11356-011-0532-2.

[18] M. Abdu, S.Babaee, A. Worku, et al, 2025. Synthesis and optimization of TiO2-biochar

composite for degradation of Basic Blue 41 dye in textile wastewater using response surface methodology. Inorganic Chemistry Communications. (2025). https://doi.org/10.1016/j.inoche.2025.114078.

[19] M. MohamedHegazy, A. KhalidHassan, Predicting the degradation of reactive red 147 dye in texti1e wastewater using response surface methodo1ogy technique, Applied Water Science. (2023). https://doi.org/10.1007/s13201-022-01826-w.

[20] Y. P. Jia, X. Q. Shan, S. X. Song, et al, Optimization of coagulation process of catering wastewater by response surface methodology, CIESC Journal. (2021). https://doi.org/10.11949/0438-1157.20210001.

[21] L.Y. Zhu, X. F. Zhou, Mn-doped DSA electrode and optimized application in water treatment process, Chemical Industry and Engineering Process. (2024). https://doi.org/10.16085/j.issn.1000-6613.2023-0860.

[22] J. Basiri Parsa, Z. Merati, M. Abbasi, Modeling and optimizing of electrochemical oxidation of CI Reactive Orange 7 on the Ti/Sb-SnO2 as anode via response surface methodology, Journal of Industrial and Engineering Chemistry. (2013). https://doi.org/10.1016/j.jiec.2012.12.039.

[23] D. Feng, Z. Shang, P. Xu, et al, 2022. Electrochemical degradation of hydrolyzed polyacrylamide by a novel La-In co-doped PbO2 electrode: Electrode characterization, influencing factors and degradation pathway. Journal of Electroanalytical Chemistry. (2022). https://doi.org/10.1016/j.jelechem.2022.116017.

[24] S. Man, D. Luo, Q. Sun, et al, 2022. When MXene (Ti3C2Tx) meet Ti/PbO2: An improved electrocatalytic activity and stability. Journal of Hazardous Materials. (2022). https://doi.org/10.1016/j.jhazmat.2022.128440.

[25] G. Dong, K. Lang, Y. Gao, et al, A novel composite anode via immobilizing of Ce-doped PbO2 on CoTiO3 for efficiently electrocatalytic degradation of dye, Journal of Colloid and Interface Science. (2022). https://doi.org/10.1016/j.jcis.2021.11.023.

[26] G. Fu, D. Butler, S. T. Khu, Multiple objective optimal control of integrated urban wastewater systems, Environmental Modelling & Software. (2008). https://doi.org/10.1016/j.envsoft.2007.06.003.

[27] S. Gao, Y. Zhang, Z.Q. Zhang, et. al, Multi-objective optimization of the combustion chamber geometry for a highland diesel engine fueled with diesel/n-butanol/PODEn by ANN-NSGA Ⅲ, Energy. (2023). https://doi.org/10.1016/j.energy.2023.128793

[28] Z. Kuang, J. Zhang, Z. Tian, et al, 2023. NSGA III based on utopian point improvements and its application in wastewater treatment process. Expert Systems with Applications. (2023). https://doi.org/10.1016/j.eswa.2023.121030.

Supplementary Files

This is a list of supplementary files associated with this preprint. Click to download.

- GraphicAbstract.docx
- Highlights.docx